JOURNAL OF SYNCHROTRON RADIATION

ISSN 1600-5775

Characterization of soft X-ray FEL pulse duration with two-color photoelectron spectroscopy

Shigeki Owada,[a,b]* Mizuho Fushitani,[c,b] Akitaka Matsuda,[c,b] Hikaru Fujise,[c,b] Yuuma Sasaki,[c,b] Yasumasa Hikosaka,[d,b] Akiyoshi Hishikawa[c,e,b] and Makina Yabashi[b,a]

[a]Japan Synchrotron Radiation Research Institute, 1-1-1 Koto, Sayo-cho, Sayo-gun, Hyogo 679-5198, Japan, [b]RIKEN SPring-8 Center, 1-1-1 Koto, Sayo-cho, Sayo-gun, Hyogo 679-5148, Japan, [c]Graduate School of Science, Nagoya University, Furo-cho, Chikusa, Nagoya, Aichi 464 8602, Japan, [d]Institute of Liberal Arts and Sciences, University of Toyama, 2630 Sugitani, Toyama 930-0194, Japan, and [e]Research Center for Materials Science, Nagoya University, Furo-cho, Chikusa, Nagoya, Aichi 464-8602, Japan. *Correspondence e-mail: osigeki@spring8.or.jp

Received 25 January 2020
Accepted 25 June 2020

Edited by Y. Amemiya, University of Tokyo, Japan

Keywords: free-electron lasers; cross-correlation; photoelectron sidebands.

The pulse duration of soft X-ray free-electron laser (FEL) pulses of SACLA BL1 (0.2–0.3 nC per bunch, 0.5–0.8 MeV) were characterized by photoelectron sideband measurements. The intensity of the He 1 s^{-1} photoelectron sidebands generated by a near-infrared femtosecond laser was measured as a function of the time delay between the two pulses using an arrival time monitor. From the width of the cross-correlation trace thus derived, the FEL pulse duration was evaluated to be 28 ± 5 fs full width at half-maximum in the photon energy range between 40 eV and 120 eV.

1. Introduction

The advent of free-electron laser (FEL) sources has promoted development of science in the extreme ultraviolet (EUV) to hard X-ray region. One of the most fundamental properties of FELs is an ultrashort pulse duration, which enables us to investigate ultrafast processes in the physical, chemical and biological fields (Young *et al.*, 2010; Boutet *et al.*, 2012; Yoneda *et al.*, 2015; Kim *et al.*, 2015; Bencivenga *et al.*, 2015; Nango *et al.*, 2016). Diagnostics of the ultrashort pulse duration are essential for investigating these dynamics, because they directly relate to the temporal resolution to be achieved.

For this purpose, several techniques in the temporal and frequency domain have been developed (Radcliffe *et al.*, 2007; Frühling *et al.*, 2009; Mitzner *et al.*, 2009; Moshammer *et al.*, 2011; Inubushi *et al.*, 2012; Grguraš *et al.*, 2012; Düsterer *et al.*, 2014; Ivanov *et al.*, 2018; Inoue *et al.*, 2019; Kubota *et al.*, 2019). In the temporal domain, one of the most straightforward methods to measure the X-ray pulse duration is cross-correlation with an optical laser. Here, an intense optical laser field produces a dressing field during the photoionization process induced by X-ray irradiation. Since the ejected photoelectrons exchange energy with the dressing field, sideband structures, which are separated from the main photoline by multiples of the optical photon energy, are generated (Glover *et al.*, 1996). Since the sideband peaks are observed only when the FEL and the optical laser pulses are temporally overlapped, the sideband intensity is monitored as a function of the delay time between the optical and X-ray pulses to create the cross-correlation trace. If the optical pulse duration is provided, the FEL pulse duration can be deconvolved from the cross-correlation trace (Azima *et al.*, 2009). The key point of this method is the accuracy of the arrival time difference between

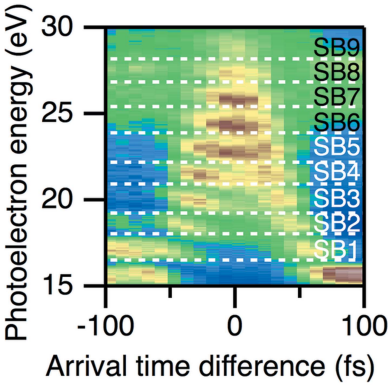

the two pulses. However, the typical arrival time jitter between the FEL and the optical laser pulses is larger than their pulse durations, which has made it difficult to retrieve the FEL pulse duration without compensation of the arrival time jitter (Meyer *et al.*, 2006). Recently, we have developed an arrival time monitor at the BL1 beamline (Owada *et al.*, 2019) of SACLA (Ishikawa *et al.*, 2012). In this study, we combined the sideband cross-correlation method with this arrival time monitor to evaluate the temporal duration of the soft X-ray FEL pulses.

2. Experimental

The experiment was performed at the endstation of SACLA BL1 [0.2–0.3 nC per bunch, 0.5–0.8 MeV (Owada *et al.*, 2018)]. The incident FEL beam ($h\nu$ = 40–120 eV, $\Delta E/E \simeq 0.02$, ~24 µJ per pulse) was introduced to a wavefront-splitting mirror (an elliptic cylindrical mirror with a sharp edge) for the arrival time diagnostic. The branched beam was focused onto a GaAs wafer to induce a transient change of the optical reflectivity, which was probed using synchronized near-infrared (NIR) pulses and detected with a visible-light CCD camera (Owada *et al.*, 2019). The arrival time differences were determined with a resolution of 15 ± 5 fs, which corresponds to a few pixels on the CCD image (Nakajima *et al.*, 2018). The remaining FEL beam and the NIR laser beam ($h\nu$ = 1.57 eV) were introduced to a vacuum chamber in an almost collinear geometry and focused onto a gaseous He target. The focus sizes of the FEL and NIR beam were ~6 µm and ~90 µm full width at half-maximum (FWHM), respectively. The temporal width of the NIR laser pulses was measured to be 28 ± 1 fs FWHM using a single-shot autocorrelation technique. The NIR pulse energy was varied from 0.1 µJ per pulse to 6.6 µJ per pulse using a half wave plate paired with a polarizer, which correspond to an NIR field intensity of 6×10^{10} W cm^{-2} and 4×10^{12} W cm^{-2}, respectively. The polarization of both lasers was horizontal, being parallel to the axis of the photoelectron flight tube. The photoelectrons produced were decelerated by a retarding electric field at the entrance of the flight tube and collected using a magnetic bottle-type electron time-of-flight (TOF) spectrometer. The high electron-collection efficiency with a 4π sterad detection angle enabled single-shot photoelectron spectroscopy (Hikosaka *et al.*, 2010; Hishikawa *et al.*, 2011; Fushitani *et al.*, 2016). During the measurement, the optical and electrical delay were fixed, whereas the actual arrival time difference between the FEL and the optical laser exhibited a jitter of ~500 fs (FWHM) (Owada *et al.*, 2019). In this study, the width of the arrival time jitter was sufficient to measure the cross-correlation between the optical and the FEL pulses without scanning an optical delay stage.

3. Results and discussion

In Fig. 1(*a*), single-shot photoelectron spectra of the He 1 s^{-1} photoelectron peak recorded with $h\nu$ = 40.8 eV and an NIR field intensity of 6.0×10^{10} W cm^{-2} are displayed against the pulse number. Although the sideband peak was not clearly formed in this figure, the sideband peaks become obvious after data sorting by the arrival time, as shown in Fig. 1(*b*). The sideband intensities from 17.5 eV to 18.1 eV are integrated and plotted as a function of arrival time difference τ, as shown in Fig. 1(*c*). The cross-correlation trace in Fig. 1(*c*) can be fitted by a Gaussian function with an FWHM width of 42 ± 1 fs.

As the NIR field intensity increases, even the second and the third sideband peaks become visible after the data sorting, as shown in Fig. 2. Since the ionization process is induced only by soft X-ray irradiation, the total electron yields were independent of the NIR pulse intensity, which means the high-order sideband generation suppresses the generation of low-order sidebands. This suppression becomes more obvious

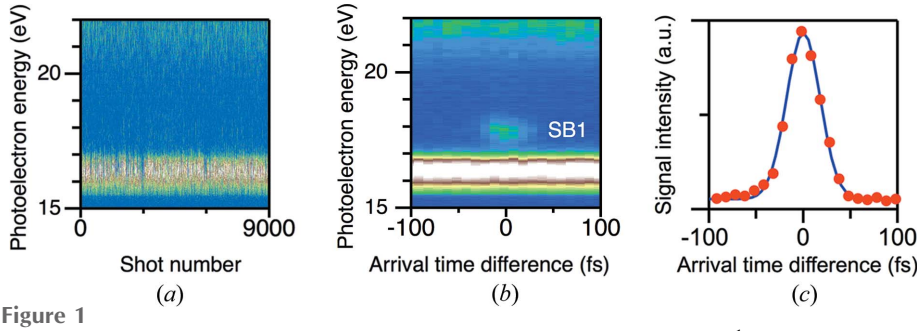

Figure 1
(*a*) Photoelectron spectra lying towards the high-energy side of the He 1 s^{-1} photoelectron line plotted with respect to the shot number. The photon energy was 40.8 eV. The NIR field intensity was 6.0×10^{10} W cm^{-2}. The background pressure of the vacuum chamber was ~1×10^{-9} Torr, and the pressure was ~1×10^{-8} Torr when the He gas was introduced to the chamber. A retarding voltage of −15 V was applied to decelerate the photoelectrons. (*b*) Averaged photoelectron spectra sorted into 10 fs time bins. SB_1 in the figure denotes the first sideband peak. (*c*) Red circles: the temporal profile of the SB_1 intensity. Blue line: Gaussian fit to the experimental data points (red circles) of the temporal profile.

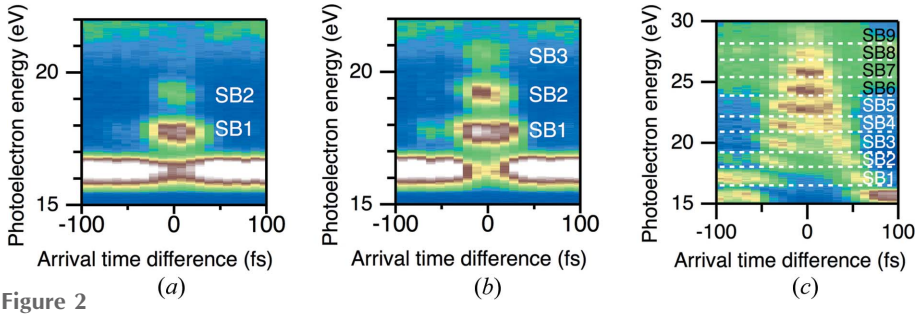

Figure 2
Photoelectron spectra at a FEL photon energy of 40.8 eV. The NIR intensities are (*a*) 1.6×10^{12} W cm^{-2}, (*b*) 4.0×10^{12} W cm^{-2} and (*c*) 8.0×10^{13} W cm^{-2}. SB_n in the figure denotes the nth sideband peak.

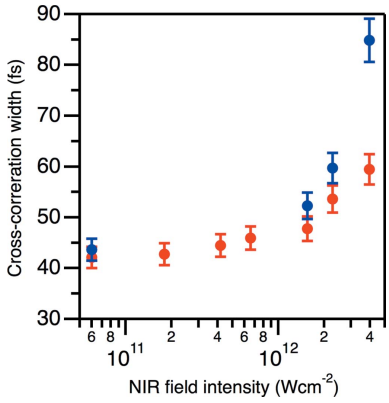

Figure 3
First-order cross-correlation (SB_1) width plotted as a function of the NIR field intensity ranging from 6.0×10^{10} W cm^{-2} to 4.0×10^{12} W cm^{-2}. Red circles: $h\nu$ = 40 eV, blue circles: $h\nu$ = 120 eV.

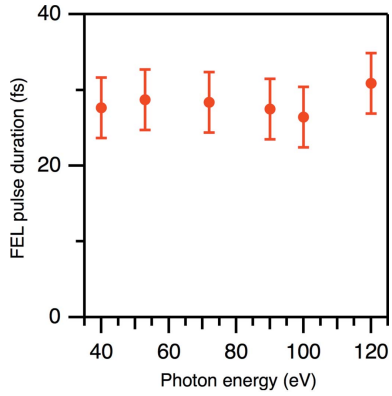

Figure 4
FEL pulse duration for various photon energies determined using an NIR laser pulse (28 fs, 6.0×10^{10} W cm^{-2}).

when the NIR intensity is 8.0×10^{13} W cm^{-2}, as shown in Fig. 2(*c*). The sidebands up to SB_9 are identified, while SB_1, SB_2 and SB_3 are completely suppressed around the zero arrival-time-difference region, where the NIR field intensity is much higher than that of the tailing region. Fig. 3 shows the first-order cross-correlation width (SB_1) plotted as a function of the NIR intensity up to 4.0×10^{12} W cm^{-2}. The figure shows that the cross-correlation width increases as the NIR field becomes more intense, because the higher order nonlinear interaction becomes significant near the zero-time delay, where the intensity of the lowest sideband (SB_1) is transferred to the higher order sidebands. This suppresses the peak of the cross-correlation trace to broaden the width. The broadening of the cross-correlation width was observed even at a higher photon energy (120 eV), as shown by the blue circles of Fig. 3. This means the NIR intensity should be as low as possible to obtain the precise FEL pulse duration. Fig. 3 shows the cross-correlation width converges at an NIR field intensity of 6.0×10^{10} W cm^{-2} for both photon energies $h\nu$ = 40.8 eV and 120 eV.

By deconvoluting the NIR pulse duration and the resolution of the arrival time monitor assuming Gaussian distribution for each envelope, the pulse duration of the soft X-ray FEL is determined as an average of fluctuating self-amplified spontaneous emission (SASE) FEL pulses. Fig. 4 shows the FEL pulse durations evaluated at an NIR field intensity of 6.0×10^{10} W cm^{-2} in the photon energy range from 40 eV to 120 eV. The FEL pulse duration is almost constant in this photon energy range, with a mean value of 28 $\pm$ 5 fs in FWHM.

Although the actual electron bunch length of SACLA BL1 has not been measured, simulations suggest that it can be longer than the FEL pulse duration determined in this work. This relationship itself is reasonable because only part of each electron bunch contributes to lasing. It should also be noted that the length of the lasing part should fluctuate from bunch to bunch and is expected to be correlated with the number of created photons, *i.e.* the pulse energy (Düsterer *et al.*, 2014; Engel *et al.*, 2016). In this study, the intensity fluctuation of the SASE-FEL pulses was ~30% in RMS, from which the fluctuation of the lasing part is estimated to be ~8 fs. SACLA BL1 is not currently equipped with any bunch compressor after the last C-band accelerator. In the near future, a set of multipole magnets will be installed for the nonlinear correction, which will enable us to investigate the relationship between the lengths of the electron bunch and the photon pulse.

4. Summary

In summary, we have evaluated the temporal duration of soft X-ray FEL pulses using time-dependent photoelectron sideband intensities. The fluctuation of the arrival time difference between the NIR and the FEL pulses was treated by resorting the photoelectron data based on arrival time monitor data. The time-dependent sideband intensity provides the precise FEL pulse duration only when the NIR intensity is sufficiently low. In this study, the FEL pulse duration was evaluated as 28 $\pm$ 5 fs in FWHM.

Acknowledgements

The authors thank all the SACLA staff for their support. The experiment was performed at SACLA with the approval of JASRI and the program review committee (proposal Nos. 2016B8018, 2017B8081, 2018A8019, 2018B8028, 2018B8097, 2019A8028 and 2019B8046).

References

Azima, A., Düsterer, S., Radcliffe, P., Redlin, H., Stojanovic, N., Li, W., Schlarb, H., Feldhaus, J., Cubaynes, D., Meyer, M., Dardis, J., Hayden, P., Hough, P., Richardson, V., Kennedy, E. T. & Costello, J. T. (2009). *Appl. Phys. Lett.* **94**, 144102.

Bencivenga, F., Cucini, R., Capotondi, F., Battistoni, A., Mincigrucci, R., Giangrisostomi, E., Gessini, A., Manfredda, M., Nikolov, I. P., Pedersoli, E., Principi, E., Svetina, C., Parisse, P., Casolari, F., Danailov, M. B., Kiskinova, M. & Masciovecchio, C. (2015). *Nature*, **520**, 205–208.

Boutet, S., Lomb, L., Williams, G. J., Barends, T. R. M., Aquila, A., Doak, R. B., Weierstall, U., DePonte, D. P., Steinbrener, J., Shoeman, R. L., Messerschmidt, M., Barty, A., White, T. A., Kassemeyer, S., Kirian, R. A., Seibert, M. M., Montanez, P. A., Kenney, C., Herbst, R., Hart, P., Pines, J., Haller, G., Gruner, S. M.,

Philipp, H. T., Tate, M. W., Hromalik, M., Koerner, L. J., van Bakel, N., Morse, J., Ghonsalves, W., Arnlund, D., Bogan, M. J., Caleman, C., Fromme, R., Hampton, C. Y., Hunter, M. S., Johansson, L. C., Katona, G., Kupitz, C., Liang, M., Martin, A. V., Nass, K., Redecke, L., Stellato, F., Timneanu, N., Wang, D., Zatsepin, N. A., Schafer, D., Defever, J., Neutze, R., Fromme, P., Spence, J. C. H., Chapman, H. N. & Schlichting, I. (2012). *Science*, **337**, 362–364.

Düsterer, S., Rehders, M., Al-Shemmary, A., Behrens, C., Brenner, G., Brovko, O., DellAngela, M., Drescher, M., Faatz, B., Feldhaus, J., Frühling, U., Gerasimova, N., Gerken, N., Gerth, C., Golz, T., Grebentsov, A., Hass, E., Honkavaara, K., Kocharian, V., Kurka, M., Limberg, Th., Mitzner, R., Moshammer, R., Plönjes, E., Richter, M., Rönsch-Schulenburg, J., Rudenko, A., Schlarb, H., Schmidt, B., Senftleben, A., Schneidmiller, E. A., Siemer, B., Sorgenfrei, F., Sorokin, A. A., Stojanovic, N., Tiedtke, K., Treusch, R., Vogt, M., Wieland, M., Wurth, W., Wesch, S., Yan, M., Yurkov, M. V., Zacharias, H. & Schreiber, S. (2014). *Phys. Rev. ST Accel. Beams*, **17**, 120702.

Engel, R., Düsterer, S., Brenner, G. & Teubner, U. (2016). *J. Synchrotron Rad.* **23**, 118–122.

Frühling, U., Wieland, M., Gensch, M., Gebert, T., Schütte, B., Krikunova, M., Kalms, R., Budzyn, F., Grimm, O., Rossbach, J., Plönjes, E. & Drescher, M. (2009). *Nat. Photon.* **3**, 523–528.

Fushitani, M., Liu, C. N., Matsuda, A., Endo, T., Toida, Y., Nagasono, M., Togashi, T., Yabashi, M., Ishikawa, T., Hikosaka, Y., Morishita, T. & Hishikawa, A. (2016). *Nat. Photon.* **10**, 102–105.

Glover, T. E., Schoenlein, R. W., Chin, A. H. & Shank, C. V. (1996). *Phys. Rev. Lett.* **76**, 2468–2471.

Grguraš, I., Maier, A. R., Behrens, C., Mazza, T., Kelly, T. J., Radcliffe, P., Düsterer, S., Kazansky, A. K., Kabachnik, N. M., Tschentscher, Th., Costello, J. T., Meyer, M., Hoffmann, M. C., Schlarb, H. & Cavalieri, A. L. (2012). *Nat. Photon.* **6**, 852–857.

Hikosaka, Y., Fushitani, M., Matsuda, A., Tseng, C. M., Hishikawa, A., Shigemasa, E., Nagasono, M., Tono, K., Togashi, T., Ohashi, H., Kimura, H., Senba, Y., Yabashi, M. & Ishikawa, T. (2010). *Phys. Rev. Lett.* **105**, 133001.

Hishikawa, A., Fushitani, M., Hikosaka, Y., Matsuda, A., Liu, C.-N., Morishita, T., Shigemasa, E., Nagasono, M., Tono, K., Togashi, T., Ohashi, H., Kimura, H., Senba, Y., Yabashi, M. & Ishikawa, T. (2011). *Phys. Rev. Lett.* **107**, 243003.

Inoue, I., Tamasaku, K., Osaka, T., Inubushi, Y. & Yabashi, M. (2019). *J. Synchrotron Rad.* **26**, 2050–2054.

Inubushi, Y., Tono, K., Togashi, T., Sato, T., Hatsui, T., Kameshima, T., Togawa, K., Hara, T., Tanaka, T., Tanaka, H., Ishikawa, T. & Yabashi, M. (2012). *Phys. Rev. Lett.* **109**, 144801.

Ishikawa, T., Aoyagi, H., Asaka, T., Asano, Y., Azumi, N., Bizen, T., Ego, H., Fukami, K., Fukui, T., Furukawa, Y., Goto, S., Hanaki, H., Hara, T., Hasegawa, T., Hatsui, T., Higashiya, A., Hirono, T., Hosoda, N., Ishii, M., Inagaki, T., Inubushi, Y., Itoga, T., Joti, Y., Kago, M., Kameshima, T., Kimura, H., Kirihara, Y., Kiyomichi, A., Kobayashi, T., Kondo, C., Kudo, T., Maesaka, H., Maréchal, X. M., Masuda, T., Matsubara, S., Matsumoto, T., Matsushita, T., Matsui, S., Nagasono, M., Nariyama, N., Ohashi, H., Ohata, T., Ohshima, T., Ono, S., Otake, Y., Saji, C., Sakurai, T., Sato, T., Sawada, K., Seike, T., Shirasawa, K., Sugimoto, T., Suzuki, S., Takahashi, S., Takebe, H., Takeshita, K., Tamasaku, K., Tanaka, H., Tanaka, R., Tanaka, T., Togashi, T., Togawa, K., Tokuhisa, A., Tomizawa, H., Tono, K., Wu, S., Yabashi, M., Yamaga, M., Yamashita, A., Yanagida, K., Zhang, C., Shintake, T., Kitamura, H. & Kumagai, N. (2012). *Nat. Photon.* **6**, 540–544.

Ivanov, R., Liu, J., Brenner, G., Brachmanski, M. & Düsterer, S. (2018). *J. Synchrotron Rad.* **25**, 26–31.

Kim, K. H., Kim, J. G., Nozawa, S., Sato, T., Oang, K. Y., Kim, T. W., Ki, H., Jo, J., Park, S., Song, C., Sato, T., Ogawa, K., Togashi, T., Tono, K., Yabashi, M., Ishikawa, T., Kim, J., Ryoo, R., Kim, J., Ihee, H. & Adachi, S. (2015). *Nature*, **518**, 385–389.

Kubota, Y., Inoue, I., Togawa, K., Kinjo, R., Iwayama, H., Harries, J. R., Inubushi, Y., Owada, S., Tono, K., Tanaka, T., Hara, T. & Yabashi, M. (2019). *Proceedings of the 16th International Conference on Megagauss Magnetic Field Generation and Related Topics (MEGAGAUSS2018)*, 25–29 September 2018, Kashiwa, Japan. Institute of Electrical and Electronics Engineers.

Meyer, M., Cubaynes, D., O'Keeffe, P., Luna, H., Yeates, P., Kennedy, E. T., Costello, J. T., Orr, P., Taïeb, R., Maquet, A., Düsterer, S., Radcliffe, P., Redlin, H., Azima, A., Plönjes, E. & Feldhaus, J. (2006). *Phys. Rev. A*, **74**, 011401.

Mitzner, R., Sorokin, A. A., Siemer, B., Roling, S., Rutkowski, M., Zacharias, H., Neeb, M., Noll, T., Siewert, F., Eberhardt, W., Richter, M., Juranic, P., Tiedtke, K. & Feldhaus, J. (2009). *Phys. Rev. A*, **80**, 025402.

Moshammer, R., Pfeifer, Th., Rudenko, A., Jiang, Y. H., Foucar, L., Kurka, M., Kühnel, K. U., Schröter, C. D., Ullrich, J., Herrwerth, O., Kling, M. F., Liu, X.-J., Motomura, K., Fukuzawa, H., Yamada, A., Ueda, K., Ishikawa, K. L., Nagaya, K., Iwayama, H., Sugishima, A., Mizoguchi, Y., Yase, S., Yao, M., Saito, N., Belkacem, A., Nagasono, M., Higashiya, A., Yabashi, M., Ishikawa, T., Ohashi, H., Kimura, H. & Togashi, T. (2011). *Opt. Express*, **19**, 21698–21706.

Nakajima, K., Joti, Y., Katayama, T., Owada, S., Togashi, T., Abe, T., Kameshima, T., Okada, K., Sugimoto, T., Yamaga, M., Hatsui, T. & Yabashi, M. (2018). *J. Synchrotron Rad.* **25**, 592–603.

Nango, E., Royant, A., Kubo, M., Nakane, T., Wickstrand, C., Kimura, T., Tanaka, T., Tono, K., Song, C., Tanaka, R., Arima, T., Yamashita, A., Kobayashi, J., Hosaka, T., Mizohata, E., Nogly, P., Sugahara, M., Nam, D., Nomura, T., Shimamura, T., Im, D., Fujiwara, T., Yamanaka, Y., Jeon, B., Nishizawa, T., Oda, K., Fukuda, M., Andersson, R., Båth, P., Dods, R., Davidsson, J., Matsuoka, S., Kawatake, S., Murata, M., Nureki, O., Owada, S., Kameshima, T., Hatsui, T., Joti, Y., Schertler, G., Yabashi, M., Bondar, A.-N., Standfuss, J., Neutze, R. & Iwata, S. (2016). *Science*, **354**, 1552–1557.

Owada, S., Nakajima, K., Togashi, T., Katayama, T., Yumoto, H., Ohashi, H. & Yabashi, M. (2019). *J. Synchrotron Rad.* **26**, 887–890.

Owada, S., Togawa, K., Inagaki, T., Hara, T., Tanaka, T., Joti, Y., Koyama, T., Nakajima, K., Ohashi, H., Senba, Y., Togashi, T., Tono, K., Yamaga, M., Yumoto, H., Yabashi, M., Tanaka, H. & Ishikawa, T. (2018). *J. Synchrotron Rad.* **25**, 282–288.

Radcliffe, P., Düsterer, S., Azima, A., Redlin, H., Feldhaus, J., Dardis, J., Kavanagh, K., Luna, H., Gutierrez, J. P., Yeates, P., Kennedy, E. T., Costello, J. T., Delserieys, A., Lewis, C. L. S., Taïeb, R., Maquet, A., Cubaynes, D. & Meyer, M. (2007). *Appl. Phys. Lett.* **90**, 131108.

Yoneda, H., Inubushi, Y., Nagamine, K., Michine, Y., Ohashi, H., Yumoto, H., Yamauchi, K., Mimura, H., Kitamura, H., Katayama, T., Ishikawa, T. & Yabashi, M. (2015). *Nature*, **524**, 446–449.

Young, L., Kanter, E. P., Krässig, B., Li, Y., March, A. M., Pratt, S. T., Santra, R., Southworth, S. H., Rohringer, N., DiMauro, L. F., Doumy, G., Roedig, C. A., Berrah, N., Fang, L., Hoener, M., Bucksbaum, P. H., Cryan, J. P., Ghimire, S., Glownia, J. M., Reis, D. A., Bozek, J. D., Bostedt, C. & Messerschmidt, M. (2010). *Nature*, **466**, 56–61.